PHYSICAL REVIEW A VOLUME 22, NUMBER 6 DECEMBER 1980

Correlation energy of open-shell systems. Application of the many-body Rayleigh-Schrödinger perturbation theory in the restricted Roothaan-Hartree-Fock formalism

Ivan Hubač
Department of Biophysics, Comenius University, 81631 Bratislava, Czechoslovakia

Petr Čársky
J. Heyrovský Institute of Physical Chemistry and Electrochemistry, Czechoslovak Academy of Sciences, 12138 Prague 2, Czechoslovakia
(Received 2 October 1979)

Correlation energy of doublet and triplet electronic states is formulated in terms of many-body diagrammatic perturbation theory through third order. Applications are presented for BH_2 and NH_2 radicals and the computed correlation energies are compared with data obtained with the same basis set from configuration-interaction treatments covering singly and doubly excited configurations. It is shown that the two approaches give correlation energies close in absolute value.

I. INTRODUCTION

Recent progress[1-4] in closed-shell correlation-energy calculations by means of many-body Rayleigh-Schrödinger perturbation theory (MB-RSPT) stimulated our attempt to find whether the same level of success may also be achieved with open-shell systems. Our goal was to formulate the method which would retain all merits of the MB-RSPT formulation of the closed-shell correlation energy. For this reason we decided to adopt the restricted Roothaan-Hartree-Fock (RHF) formalism[5] and to apply it to MB-RSPT through third order. Although the use of the unrestricted Hartree-Fock (UHF) formalism affords a straightforward formulation[6] of the problem, the necessity of handling two sets of orbitals (with α and β spins) brings about considerable storage requirements and computational effort. A disagreeable circumstance encountered in configuration-interaction treatments covering singly and doubly excited configurations (CI-SD) is the rapidly increasing number of configurations (considerably more than with closed-shell systems) as the size of the basis set is increased. Another disadvantage of the open-shell CI-SD, as of course of any CI-SD approach, is the size inconsistency.[6-8] It was our opinion that MB-RSPT in the RHF formalism might avoid all above-mentioned drawbacks. A point in favor for UHF approach was raised recently by Roos and Siegbahn[9] who showed that UHF-CI-SD calculations are superior to RHF-CI-SD calculations for systems far from the equilibrium geometry. We tend to believe, however, that the use of the RHF approach might be profitable even in this case. The experience accumulated with closed-shell MB-RSPT treatments suggests that a justifiable preselection of important terms from higher orders of MB-RSPT should also be tractable for open-shell systems. With the use of this specific and appealing feature of MB-RSPT, the drawback of the RHF approach should be eliminated.

II. THEORY

The most important concept of MB-RSPT is the normal product form of the Hamiltonian. Using the second quantization formalism we can write the Hamiltonian

$$H = Z + V, \tag{1}$$

where Z and V are its one- and two-particle components, respectively, in the normal product form as follows:

$$H = \langle \Phi_0 | H | \Phi_0 \rangle + \sum_{AB} \langle A | f | B \rangle N[X_A^\dagger X_B] + \tfrac{1}{2} \sum_{ABCD} \langle AB | v | CD \rangle N[X_A^\dagger X_B^\dagger X_D X_C]. \tag{2}$$

Here $X_A^\dagger(X_B)$ are creation (annihilation) operators defined on the one-particle spin-orbital basis set $|A\rangle, |B\rangle \ldots, N[\cdots]$ is the normal product of creation and annihilation operators, operator f is the Hartree-Fock operator

$$f = h + \sum_{i=1}^{\text{occ}} (J_{A_i} - K_{A_i}), \tag{3}$$

v is the electronic-repulsion operator and $|\Phi_0\rangle$ is the Slater determinant given as

$$|\Phi_0\rangle = \prod_{i=1}^{\text{occ}} X_{A_i}^\dagger |0\rangle. \tag{4}$$

The open-shell RHF method developed by Roothaan[5] can accommodate certain types of open-shell configurations. We shall restrict ourselves here to the most common of them, viz., to those that may be referred to as the half-closed-shell case.[5] Examples of half-closed-shell systems are nondegenerate doublet states that are the lowest in

energy for a given symmetry, the ground triplet state of the O_2 molecule, the lowest triplet state of any closed-shell molecule if the excitation is from a nondegenerate to a nondegenerate orbital, the atomic $N\,^4S$ state, and the $a\,^4\Sigma^-$ state of the CH radical ($3\sigma 1\pi^2$ configuration). A characteristic feature of all these states is the open shell consisting of singly occupied, complete degenerate sets of orbitals with all the spins being parallel. The respective Hartree-Fock operator, f_R, has the following form:

$$f_R = h + \sum_{a\in D}(2J_a - K_a) + \sum_{m\in S}(J_m - \tfrac{1}{2}K_m) + P_T Q + Q P_T - Q\,, \tag{5}$$

where the operators P_T and Q are defined as

$$Q = \sum_{m\in S} K_m\,, \tag{6}$$

$$P_T = \sum_{a\in D} |a\rangle\langle a| + \tfrac{1}{2}\sum_{m\in S} |m\rangle\langle m|\,. \tag{7}$$

Here the summation over D means that both spin orbitals $|a\rangle|\alpha\rangle \equiv |A\rangle$ and $|a\rangle|\beta\rangle \equiv |B\rangle$ are included in $|\Phi_0\rangle$, and the summation over S means that spin orbitals $|m\rangle|\alpha\rangle$ are included in $|\Phi_0\rangle$ and that $|m\rangle|\beta\rangle$ belong to unoccupied spin orbitals. Hereafter we use consistently lower-case characters for orbitals and capital letters for spin orbitals. In this notation the f_R operator (5) over spin orbitals becomes

$$f_R^\alpha = h + \sum_{A\in D_\alpha}(J_A - K_A) + \sum_{B\in D_\beta} J_B + \tfrac{1}{2}\sum_{M\in S_\alpha}(J_M - K_M) + \tfrac{1}{2}\sum_{N\in S_\beta} J_N + P_T^\alpha Q^\alpha + Q^\alpha P_T^\alpha - Q^\alpha\,, \tag{8}$$

for α spins and

$$f_R^\beta = h + \sum_{A\in D_\beta}(J_A - K_A) + \sum_{B\in D_\alpha} J_B + \tfrac{1}{2}\sum_{M\in S_\alpha} J_M + \tfrac{1}{2}\sum_{N\in S_\beta}(J_N - K_N) + P_T^\beta Q^\beta + Q^\beta P_T^\beta - Q^\beta\,, \tag{9}$$

for β spins.

Now the application of MB-RSPT to the RHF approximation means that we have to express the operator $f_R(5)$ in the form[10]

$$f_R = f + U\,, \tag{10}$$

where f is given by Eq. (3) and U is some new one-particle operator. The form of the latter depends on the particular case of the electronic configuration. Considering

$$|\Phi_0\rangle = \prod_{a\in D} X^\dagger_{a,\alpha} X^\dagger_{a,\beta} \prod_{m\in S} X^\dagger_{m,\alpha}|0\rangle\,, \tag{11}$$

the general form of U can be obtained by subtracting the operator f from f_R. Thus, substituting Eqs. (3) and (8) into (10) gives us

$$U^\alpha = \left(h + \sum_{A\in D_\alpha}(J_A - K_A) + \sum_{B\in D_\beta} J_B + \tfrac{1}{2}\sum_{M\in S_\alpha}(J_M - K_M) + \tfrac{1}{2}\sum_{N\in S_\beta} J_N + P_T^\alpha Q^\alpha + Q^\alpha P_T^\alpha - Q^\alpha\right) - \left(h + \sum_{A\in D_\alpha}(J_A - K_A) + \sum_{M\in S_\alpha}(J_M - K_M) + \sum_{B\in D_\beta} J_B\right). \tag{12}$$

On applying U^α to a spin orbital $|A\rangle \equiv |a\rangle|\alpha\rangle$, we obtain

$$U^\alpha|A\rangle = \left[\left(\tfrac{1}{2}\sum_{N\in S_\beta} J_N + P_T^\alpha Q^\alpha + Q^\alpha P_T^\alpha - Q^\alpha\right) - \tfrac{1}{2}\sum_{M\in S_\alpha}(J_M - K_M)\right]|A\rangle\,, \tag{13}$$

which gives us

$$U^\alpha = \tfrac{1}{2}\sum_{M\in S_\alpha} K_M + P_T^\alpha Q^\alpha + Q^\alpha P_T^\alpha - Q^\alpha\,. \tag{14}$$

Similarly, by substituting into Eq. (10) from (3) and (9), we obtain

$$U^\beta = \left(h + \sum_{A\in D_\beta}(J_A - K_A) + \sum_{B\in D_\alpha} J_B + \tfrac{1}{2}\sum_{M\in S_\alpha} J_M + \tfrac{1}{2}\sum_{N\in S_\beta}(J_N - K_N) + P_T^\beta Q^\beta + Q^\beta P_T^\beta - Q^\beta\right) - \left(h + \sum_{B\in D_\beta}(J_B - K_B) + \sum_{A\in D_\alpha} J_A + \sum_{M\in S_\alpha} J_M\right). \tag{15}$$

On applying U^β to a spin orbital $|B\rangle \equiv |b\rangle|\beta\rangle$ we obtain

$$U^\beta|B\rangle = \left(\tfrac{1}{2}\sum_{N\in S_\beta}(J_N - K_N) - \tfrac{1}{2}\sum_{M\in S_\alpha} J_M + P_T^\beta Q^\beta + Q^\beta P_T^\beta - Q^\beta\right)|B\rangle\,, \tag{16}$$

which gives us

$$U^{\beta} = -\tfrac{1}{2} \sum_{N \in S_{\beta}} K_N + P_T^{\beta} Q^{\beta} + Q^{\beta} P_T^{\beta} - Q^{\beta} . \quad (17)$$

Combining U^{α} and U^{β} we arrive at the final form of the U operator

$$U = \tfrac{1}{2} \sum_{M \in S_{\alpha}} K_M - \tfrac{1}{2} \sum_{N \in S_{\beta}} K_N + P_T Q + Q P_T - Q . \quad (18)$$

Once the expression for U is available,[11] it is possible to rewrite the Hamiltonian (2) in the form

$$H = \langle \Phi_0 | H | \Phi_0 \rangle + \sum_A \epsilon_A N[X_A^{\dagger} X_A] + \tfrac{1}{2} \sum_{ABCD} \langle AB | v | CD \rangle N[X_A^{\dagger} X_B^{\dagger} X_D X_C] - \sum_{AB} \langle A | u | B \rangle N[X_A^{\dagger} X_B] , \quad (19)$$

where ϵ_A are the eigenvalues of the f_R operator.

The actual calculations of the correlation energy of open-shell systems by means of MB-RSPT can be made along the same lines as for the closed-shell systems.[12,13] We define

$$K | \Psi_0 \rangle = k | \Psi_0 \rangle , \quad (20)$$

$$K = H - \langle \Phi_0 | H | \Phi_0 \rangle , \quad (21)$$

as the perturbed (exact) eigenvalue problem and

$$K_0 | \Phi_0 \rangle = k_0 | \Phi_0 \rangle , \quad (22)$$

$$K_0 = H_0 - \langle \Phi_0 | H_0 | \Phi_0 \rangle , \quad (23)$$

as the unperturbed eigenvalue problem, and

$$K = K_0 + W - U . \quad (24)$$

Comparing Eqs. (19), (21), and (24) we obtain

$$W = \tfrac{1}{2} \sum_{ABCD} \langle AB | v | CD \rangle N[X_A^{\dagger} X_B^{\dagger} X_D X_C] \quad (25)$$

and

$$U = \sum_{AB} \langle A | u | B \rangle N[X_A^{\dagger} X_B] . \quad (26)$$

By means of the Rayleigh-Schrödinger perturbation expansion through third order we can write[12,13]

$$k = \langle \Phi_0 | (W - U) Q_0 (W - U) | \Phi_0 \rangle + \langle \Phi_0 | (W - U) Q_0 (W - U) Q_0 (W - U) | \Phi_0 \rangle , \quad (27)$$

where the first term on the right-hand side of Eq. (27) represents the second-order contribution to the correlation energy, $k^{(2)}$, and the second term of Eq. (27) the third-order contribution, $k^{(3)}$.

Let us assign the diagrams to the following mathematical expressions (see Ref. 13):

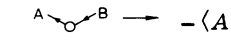

$$\longrightarrow \; - \langle A | u | B \rangle N[X_A^{\dagger} X_B] \quad (28)$$

and

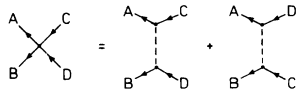

, (29)

where

$$\longrightarrow \; \langle AB | v | CD \rangle N[X_A^{\dagger} X_B^{\dagger} X_D X_C] . \quad (30)$$

Following the diagrammatic rules[12,13] we can arrive at the diagrams entered in Fig. 1, which gives the diagrammatic representation of Eq. (27).

A. Nondegenerate doublet state

For this case the form of the wave function (11) becomes

$$| \Phi_0 \rangle = \left(\prod_{a \in D} X_{a,\alpha}^{\dagger} X_{a,\beta}^{\dagger} \right) X_{m,\alpha}^{\dagger} | 0 \rangle \quad (31)$$

and the U operator (18) reduces to

$$U = \tfrac{1}{2} K_{m,\alpha} - \tfrac{1}{2} K_{m,\beta} + P_T Q + Q P_T - Q . \quad (32)$$

In order to be able to evaluate the whole expression for the correlation energy (27) over orbitals we need to know how to evaluate the matrix elements

$$\langle A | u | B \rangle = \delta_{\alpha\beta} F(\rho; a, b) \langle a | K_m | b \rangle . \quad (33)$$

The value of the factor $F(\rho; a, b)$ depends on the nature of the spin orbitals $|A\rangle = |a\rangle | \alpha \rangle$ and $|B\rangle$

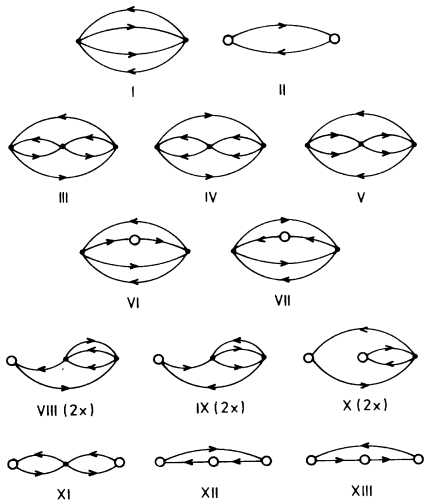

FIG. 1. Hugenholtz diagrams for the second-order (I, II) and the third-order (III–XIII) contributions to the correlation energy of half-closed-shell systems. The diagrams VIII, IX, and X can be obtained in two topologically different ways and their contributions must therefore be counted twice.

$= |b\rangle|\beta\rangle$. The nine possible cases for α spins are presented in Table I. The factors for β spins can be obtained simply by subtracting 1 from the factor $F(\alpha; a, b)$; i.e.,

$$F(\beta; a, b) = F(\alpha; a, b) - 1 . \tag{34}$$

The explicit expressions for diagrams I–XIII were obtained by means of diagrammatic rules reported previously.[13] The respective formulas are summarized in the Appendix.

It should be noted that the theory in the form given in this section may also be applied to degenerate doublet states, such as e.g., $1/\sqrt{2}(|m^2n| + |mn^2|)$ state, assuming $|\Phi_0\rangle$ as a single determinant $|m^2n|$ and assigning to it the wave function given by Eq. (31).

B. Triplet states

The theoretical approach presented above may also be applied to triplet-state configurations in which a twofold-degenerate molecular orbital is filled with two electrons (e.g., the ground state of the O_2 molecule) or to excited triplet states in which the electron is promoted from a nondegenerate orbital to a nondegenerate orbital. These two types of configurations may be expressed by the following wave function:

$$|\Phi_0\rangle = \left(\prod_{a\in D} X^{\dagger}_{a,\alpha} X^{\dagger}_{a,\beta}\right) X^{\dagger}_{m,\alpha} X^{\dagger}_{n,\alpha} |0\rangle . \tag{35}$$

Note that instead of the usual spin function $(1/\sqrt{2})(\alpha\beta + \beta\alpha)$ we use the spin function $\alpha\alpha$, which is more convenient for our purposes. In this case the U operator (18) reduces to

$$U = \tfrac{1}{2} K_{m,\alpha} + \tfrac{1}{2} K_{n,\alpha} - \tfrac{1}{2} K_{m,\beta} - \tfrac{1}{2} K_{n,\beta} + P_T Q + Q P_T - Q , \tag{36}$$

and the matrix elements of the operator can be expressed as

$$\langle A|u|B\rangle = \delta_{\alpha\beta} F(\rho; a, b)(\langle a|K_m|b\rangle + \langle a|K_n|b\rangle) . \tag{37}$$

The factors $F(\alpha; a, b)$ are the same as in Table I and, for $F(\beta; a, b)$ factors, Eq. (34) holds.

TABLE I. Spin factors $F(\alpha; a, b)$ for the matrix elements $\langle A|u|B\rangle$. D, S, and V, respectively, mean doubly occupied, singly occupied, and virtual orbitals.

	$a\in D$	$a\in S$	$a\in V$
$b\in D$	$\frac{3}{2}$	1	$\frac{1}{2}$
$b\in S$	1	$\frac{1}{2}$	0
$b\in V$	$\frac{1}{2}$	0	$-\frac{1}{2}$

C. The use of the half-electron operator

From the point of view of computational feasibility we consider it expedient to make a short note on a different partitioning of the Hamiltonian, viz., on the use of the half-electron operator[14,15]:

$$f_H = h + \sum_{a\in D} (2J_a - K_a) + \tfrac{1}{2} \sum_{m\in S} (2J_m - K_m) . \tag{38}$$

An appealing feature of the half-electron approach is much better convergence of the self-consistent-field (SCF) procedure than that of the Roothaan open-shell procedure. Sometimes it is difficult to achieve the convergence with the Roothaan method, whereas the use of the half-electron method makes such a case tractable. Moreover, if use is made of the half-electron approach, the evaluation of certain diagrams also becomes easier.

Following the procedure described for the doublet state, we find that the expression for the U operator reduces to

$$U = \tfrac{1}{2} \sum_{M\in S_\alpha} K_M - \tfrac{1}{2} \sum_{N\in S_\beta} K_N \tag{39}$$

and its matrix elements are simply given by

$$\langle A|u|B\rangle = \delta_{\alpha\beta} F(\rho; a, b)\langle a|Q|b\rangle , \tag{40}$$

where $F(\alpha; a, b) = 1$ and $F(\beta; a, b) = -1$.

III. APPLICATIONS TO BH_2 AND NH_2 RADICALS

In order to test the utility of the theoretical approach described in Sec. II we selected a few reported RHF-CI calculations and repeated them with the MB-RSPT approach using the same SCF reference state, basis set, and the molecular geometry. The systems treated were BH_2 and NH_2 in their ground and lowest-excited-doublet states for which CI calculations covering all singly and doubly excited configurations (CI-SD) were reported.[16,17] The calculated correlation energies are valence-shell correlation energies, because the $1a_1$ orbital was kept doubly occupied. Two basis sets were used. The smaller of the two, of the double zeta quality (DZ), was the Dunning's[18] [4s2p/2s] contraction of the Huzinaga's[19] (9s5p/4s) primitive Gaussian set. The hydrogen s functions were scaled by the factor $1.2^2 = 1.44$. A larger basis set (DZ+P) was augmented with a set of six Gaussian d functions centered on the heavy atom and a single set of p functions on hydrogen atoms. The following exponents were used: 0.7 for B, 0.75 for N, and 1.0 for H. The geometries assumed are given in Table II. In Table III we compare our MB-RSPT results with the reported CI-SD calculations, and in Table IV we present the contributions from the diagrams I–XIII for a par-

TABLE II. Geometries assumed.[a]

Molecule	State	Basis set	r (Å)	(deg)
BH_2	$^2A_1$	DZ	1.1906[b]	135.0[b]
BH_2	$^2B_1$	DZ	1.1906[b]	135.0[b]
NH_2	$^2B_1$	DZ	1.0439	108.37
NH_2	$^2A_1$	DZ	1.0086	144.76
BH_2	$^2A_1$	DZ + P	1.1893	129.48
NH_2	$^2B_1$	DZ + P	1.0289	103.08
NH_2	$^2A_1$	DZ + P	0.9997	143.35

[a] Taken from Ref. 17 unless otherwise noted.
[b] Reference 16.

ticular case of the NH_2 radical in the $^2B_1$ ground state.

IV. DISCUSSION

A comparison of CI-SD and MB-RSPT results exhibits some similar features as the analysis reported recently for closed-shell molecules.[20] First, MB-RSPT gives us approximately 100% of the correlation energy as compared to CI-SD results. Second, the amount of the correlation energy depends slightly on the size of the basis set, the coverage being several per cent higher with the DZ + P basis set than with the DZ basis set. Third, we found that the third-order contribution may be rather large. Among the closed-shell systems treated previously,[20] a large third-order contribution was found with the BH molecule; here this is the case of the BH_2 radical. Table III shows that the correlation energy recovered ranges from 96.2% to 102.9% with respect to the correlation energy given by CI-SD calculations. A higher percentage achieved with MB-RSPT in some cases does not imply, of course, that the MB-RSPT result is more accurate than the CI one. Actually, the comparison is encumbered by the fact that MB-RSPT is not an energy minimization process, whereas CI is a genuine variational method. However, a point in favor of MB-RSPT is that this approach is size consistent, whereas CI-SD is not. Size inconsistency of CI-SD is due to a spurious term contained in the CI-SD energy, which has an unphysical nonlinear dependence on the number of electrons.[7] This prevents one from comparing effectively the CI-SD energies for molecules of different size.[6] Thus, the entries of Table III merely suggest that, in actual applications, MB-RSPT through third order and CI-SD should give similar results. It is the authors' opinion that MB-RSPT might be the preferred method in applications to open-shell systems because of a lower cost. For a given size of the basis set, the number of doubly excited configurations for the open-shell ground state is considerably higher than it is for the closed-shell ground state. With MB-RSPT the respective difference does not appear to be so important. Actually, the restricted molecular orbital open-shell MB-RSPT calculations may be performed at a cost only moderately higher than the ordinary closed-shell MB-RSPT calculations.

Let us now comment on the individual contributions of diagrams I–XIII. The entries in Table IV represent a typical result obtained for the series of systems treated in this paper. As it is seen, the prevailing contribution to the correlation energy is due to the second-order diagram I. The other second-order diagram II gives a rather small contribution. Among the third-order diagrams, the important contributions are due to diagrams III, IV, V, VI, and VII. For numerical reasons, the contributions from diagrams with two or more u vertices are negligible (at least for the systems treated). The same holds for the diagrams with one u vertex with one particle line and one hole line (diagrams VIII, IX). This finding might be of importance for a possible extension of MB-RSPT to higher orders. It seems hopeful that the number of diagrams in fourth order might be

TABLE III. Comparison of MB-RSPT and CI-SD valence-shell correlation energies (in a.u.).

Molecule	State	Basis set	SCF	CI-SD[a]	MB-RSPT $k^{(2)}$	MB-RSPT $k^{(2)}+k^{(3)}$	$\frac{k^{(2)}+k^{(3)}}{\text{(CI-SD)}}$ (%)
BH_2	$^2A_1$	DZ	−25.739 58[b]	−0.050 58[b]	−0.040 42	−0.048 68	96.2
BH_2	$^2B_1$	DZ	−25.698 51[b]	−0.056 96[b]	−0.045 24	−0.054 83	96.3
NH_2	$^2B_1$	DZ	−55.543 648	−0.099 05	−0.095 55	−0.098 57	99.5
NH_2	$^2A_1$	DZ	−55.504 962	−0.094 25	−0.092 34	−0.093 87	99.6
BH_2	$^2A_1$	DZ + P	−25.752 516	−0.080 69	−0.072 36	−0.082 93	102.8
NH_2	$^2B_1$	DZ + P	−55.573 224	−0.160 83	−0.161 33	−0.165 46	102.9
NH_2	$^2A_1$	DZ + P	−55.523 338	−0.156 81	−0.157 99	−0.161 33	102.9

[a] Reference 17 unless otherwise noted.
[b] Reference 16.

TABLE IV. Contributions from diagrams I–XIII to the correlation energy of the NH_2 radical in the $^2B_1$ ground state given by the DZ +P basis set.

Diagram	Energy (a.u.)	Diagram	Energy (a.u.)
I	−0.158 30	VIII	0.000 81
II	−0.003 02	IX	0.000 40
III	−0.090 43	X	−0.000 11
IV	0.036 19	XI	−0.000 95
V	0.033 65	XII	0.000 17
VI	0.009 99	XIII	0.000 18
VII	0.005 96		

considerably reduced under a numerical control. Specifically, one can anticipate that only the following fourth-order diagrams will be important: twelve double-excitation diagrams,[2] diagrams A through D2 (notation of Ref. 3), and diagrams containing one u vertex with two particle lines or two hole lines (the fourth-order analogs of diagrams VI and VII). In this way it is possible to expect that the RHF approximation can provide the same level of accuracy[9] as the UHF approximation in applications to structures far from the equilibrium geometry.

ACKNOWLEDGMENTS

Our computer program is largely based on the program written by Dr. M. Urban and Dr. V. Kellö (Ref. 20) for closed-shell MB-RSPT calculations. It is a pleasure to acknowledge the profit from having had their program available.

APPENDIX

Here we present the explicit formulas for diagrams I–XIII over spin orbitals generated by the RHF-SCF procedure for nondegenerate doublet states. The electronic-repulsion integrals are given here in Parr's $(11|22)$ notation, in contrast to the text where use is made of Dirac's $\langle 12|12\rangle$ notation; since the former is more suitable for computer programming whereas the latter conforms to the MB-RSPT formulation. Singly and doubly primed indices, respectively, refer to occupied and virtual spin orbitals. For meaning of $\langle A|u|B\rangle$ elements see Eqs. (33) and (34) and Table I. The expressions for diagrams VIII–X involve the factor of 2 noted in Fig. 1.

Diagram I:

$$\tfrac{1}{2}\sum_{A''B''I'J'}(A''I'|B''J')\frac{1}{\epsilon_{I'}+\epsilon_{J'}-\epsilon_{A''}-\epsilon_{B''}}[(A''I'|B''J')-(A''J'|B''I')]\,. \tag{A1}$$

Diagram II:

$$\sum_{A''I'}\langle I'|u|A''\rangle\frac{1}{\epsilon_{I'}-\epsilon_{A''}}\langle A''|u|I''\rangle\,. \tag{A2}$$

Diagram III:

$$\sum_{A''B''C''I'J'K'}[(A''I'|C''K')-(A''K'|C''I')]\frac{1}{\epsilon_{I'}+\epsilon_{K'}-\epsilon_{A''}-\epsilon_{C''}}\times[(B''J'|C''K')-(B''C''|J'K')]\frac{1}{\epsilon_{I'}+\epsilon_{J'}-\epsilon_{A''}-\epsilon_{B''}}[(A''I'|B''J')-(A''J'|B''I')]\,. \tag{A3}$$

Diagram IV:

$$\tfrac{1}{2}\sum_{A''B''C''D''I'J'}(A''I'|B''J')\frac{1}{\epsilon_{I'}+\epsilon_{J'}-\epsilon_{A''}-\epsilon_{B''}}(A''C''|B''D'')\frac{1}{\epsilon_{I'}+\epsilon_{J'}-\epsilon_{C''}-\epsilon_{D''}}[(C''I'|D''J')-(C''J'|D''I')]\,. \tag{A4}$$

Diagram V:

$$\tfrac{1}{2}\sum_{A''B''I'J'K'L'}(A''I'|B''J')\frac{1}{\epsilon_{I'}+\epsilon_{J'}-\epsilon_{A''}-\epsilon_{B''}}(I'K'|J'L')\frac{1}{\epsilon_{K'}+\epsilon_{L'}-\epsilon_{A''}-\epsilon_{B''}}[(A''K'|B''L')-(A''L'|B''K')]\,. \tag{A5}$$

Diagram VI:

$$\sum_{A''B''I'J'K'}(A''I'|B''J')\frac{1}{\epsilon_{I'}+\epsilon_{J'}-\epsilon_{A''}-\epsilon_{B''}}\langle K'|u|I'\rangle\frac{1}{\epsilon_{K'}+\epsilon_{J'}-\epsilon_{A''}-\epsilon_{B''}}[(B''J'|A''K')-(B''K'|A''J')]\,. \tag{A6}$$

Diagram VII:

$$\sum_{A''B''C''I'J'} (A''I'|B''J') \frac{1}{\epsilon_{I'}+\epsilon_{J'}-\epsilon_{A''}-\epsilon_{B''}} \langle B''|u|C''\rangle \frac{1}{\epsilon_{I'}+\epsilon_{J'}-\epsilon_{A''}-\epsilon_{C''}} [(A''J'|C''I')-(A''I'|C''J')] . \quad \text{(A7)}$$

Diagram VIII:

$$2 \sum_{A''B''C''I'J'} (A''I'|B''J') \frac{1}{\epsilon_{I'}+\epsilon_{J'}-\epsilon_{A''}-\epsilon_{B''}} \langle C''|u|I'\rangle \frac{1}{\epsilon_{I'}-\epsilon_{C''}} [(A''J'|B''C'')-(A''C''|B''J')] . \quad \text{(A8)}$$

Diagram IX:

$$2 \sum_{A''B''I'J'K'} (A''I'|B''J') \frac{1}{\epsilon_{I'}+\epsilon_{J'}-\epsilon_{A''}-\epsilon_{B''}} \langle B''|u|K'\rangle \frac{1}{\epsilon_{K'}-\epsilon_{B''}} [(A''I'|K'J')-(A''J'|K'I')] . \quad \text{(A9)}$$

Diagram X:

$$-2 \sum_{A''B''I'J'} (A''I'|B''J') \frac{1}{\epsilon_{I'}+\epsilon_{J'}-\epsilon_{A''}-\epsilon_{B''}} \langle B''|u|I'\rangle \frac{1}{\epsilon_{J'}-\epsilon_{A''}} \langle A''|u|J'\rangle . \quad \text{(A10)}$$

Diagram XI:

$$-\sum_{A''B''I'J'} \langle A''|u|I'\rangle \frac{1}{\epsilon_{I'}-\epsilon_{A''}} (A''B''|I'J') \frac{1}{\epsilon_{J'}-\epsilon_{B''}} \langle B''|u|J'\rangle . \quad \text{(A11)}$$

Diagram XII:

$$-\sum_{A''B''I'} \langle I'|u|A''\rangle \frac{1}{\epsilon_{I'}-\epsilon_{A''}} \langle A''|u|B''\rangle \frac{1}{\epsilon_{I'}-\epsilon_{B''}} \langle B''|u|I'\rangle . \quad \text{(A12)}$$

Diagram XIII:

$$\sum_{A''I'J'} \langle A''|u|I'\rangle \frac{1}{\epsilon_{I'}-\epsilon_{A''}} \langle I'|u|J'\rangle \frac{1}{\epsilon_{J'}-\epsilon_{A''}} \langle J'|u|A''\rangle . \quad \text{(A13)}$$

For computational reasons it is profitable to have the expressions in the orbital form. Below are listed the formulas for diagrams for which this is simply achievable. For the others the evaluation through orbitals is troublesome. In our computer program, we considered it, therefore, preferable to evaluate the diagrams I and III–VII according to formulas (A1) and (A3)–(A7) over spin orbitals using a list of integrals over orbitals and an auxiliary one-dimensional array for the orbital–spin-orbital index interconversion.

Diagram II:

$$\tfrac{1}{2} \sum_{a''\in V,\, i'\in D} (a''m|mi') \frac{1}{\epsilon_{i'}-\epsilon_{a''}} (i'm|ma'') . \quad \text{(A14)}$$

Diagram VIII:

$$\sum_{a''b''c''i'j'} (a''i'|b''j') \frac{1}{\epsilon_{i'}+\epsilon_{j'}-\epsilon_{a''}-\epsilon_{b''}} (c''m|mi') \frac{1}{\epsilon_{i'}-\epsilon_{c''}} [2p(a''c''|b''j')-q(a''j'|b''c'')] , \quad \text{(A15)}$$

where the values of p and q are given in Table V.

Diagram IX:

$$\sum_{a''b''i'j'k'} (a''i'|b''j') \frac{1}{\epsilon_{i'}+\epsilon_{j'}-\epsilon_{a''}-\epsilon_{b''}} (b''m|mk') \frac{1}{\epsilon_{k'}-\epsilon_{b''}} [2p(a''i'|k'j')-q(a''j'|k'i')] , \quad \text{(A16)}$$

where the values of p and q are given in Table VI.

TABLE V. Values of p and q in formula (A15).

p	q	Orbital occupation				
1	1	$i'\in D$,	$j'\in D$,	$a''\in S$,	$b''\in V$,	$c''\in V$
0	1	$i'\in D$,	$j'\in D$,	$a''\in V$,	$b''\in S$,	$c''\in V$
0	−1	$i'\in D$,	$j'\in S$,	$a''\in V$,	$b''\in V$,	$c''\in V$
$\frac{1}{2}$	0	$i'\in D$,	$j'\in S$,	$a''\in S$,	$b''\in V$,	$c''\in V$
0	0	all other cases				

TABLE VI. Values of p and q in formula (A16).

p	q	Orbital occupation				
1	1	$i'\in D$,	$j'\in S$,	$k'\in D$,	$a''\in V$,	$b''\in V$
0	1	$i'\in S$,	$j'\in D$,	$k'\in D$,	$a''\in V$,	$b''\in V$
0	−1	$i'\in D$,	$j'\in D$,	$k'\in D$,	$a''\in S$,	$b''\in V$
$\frac{1}{2}$	0	$i'\in D$,	$j'\in S$,	$k'\in D$,	$a''\in S$,	$b''\in V$
0	0	all other cases				

Diagram X:

$$-\sum_{a'',b''\in V,i',j'\in D}(a''i'|b''j')\frac{1}{\epsilon_{i'}+\epsilon_{j'}-\epsilon_{a''}-\epsilon_{b''}}(b''m|mi')\frac{1}{\epsilon_{j'}-\epsilon_{a''}}(a''m|mj'). \tag{A17}$$

Diagram XI:

$$-\tfrac{1}{2}\sum_{a'',b''\in V,i',j'\in D}(a''m|mi')\frac{1}{\epsilon_{i'}-\epsilon_{a''}}(a''b''|i'j')\frac{1}{\epsilon_{j'}-\epsilon_{b''}}(b''m|mj'). \tag{A18}$$

Diagram XII:

$$\tfrac{1}{2}\sum_{a'',b''\in V,i'\in D}(i'm|ma'')\frac{1}{\epsilon_{i'}-\epsilon_{a''}}(a''m|mb'')\frac{1}{\epsilon_{i'}-\epsilon_{b''}}(b''m|mi'). \tag{A19}$$

Diagram XIII:

$$\tfrac{1}{2}\sum_{a''\in V,i',j'\in D}(a''m|mi')\frac{1}{\epsilon_{i'}-\epsilon_{a''}}(i'm|mj')\frac{1}{\epsilon_{j'}-\epsilon_{a''}}(j'm|ma''). \tag{A20}$$

[1]R. Krishnan and J. A. Pople, Int. J. Quantum Chem. 14, 91 (1978).
[2]R. J. Bartlett and G. D. Purvis, Int. J. Quantum Chem. 14, 561 (1978).
[3]I. Hubač, M. Urban, and V. Kellö, Chem. Phys. Lett. 62, 584 (1979).
[4]S. Wilson and D. M. Silver, Mol. Phys. 36, 1539 (1978).
[5]C. C. J. Roothaan, Rev. Mod. Phys. 32, 179 (1960).
[6]J. A. Pople, J. S. Binkley, and R. Seeger, Int. J. Quantum Chem. Symp. 10, 1 (1976).
[7]A. Meunier, B. Levy, and G. Berthier, Int. J. Quantum Chem. 10, 1061 (1976).
[8]R. J. Bartlett and D. M. Silver, Int. J. Quantum Chem. Symp. 9, 183 (1975).
[9]B. O. Roos and P. E. M. Siegbahn, in *Modern Theoretical Chemistry*, edited by H. F. Schaefer III (Plenum, New York, 1977), Vol. 3, p. 277.
[10]L. S. Cederbaum and J. Schirmer, Z. Phys. 271, 221 (1974).
[11]V. Kvasnička and I. Hubač (unpublished).
[12]J. Paldus and J. Čížek, Adv. Quantum Chem. 9, 105 (1975).
[13]I. Hubač and P. Čársky, Top. Curr. Chem. 75, 97 (1978).
[14]H. C. Longuet-Higgins and J. A. Pople, Proc. Phys. Soc. London 68A, 591 (1955).
[15]F. O. Ellison and F. M. Matheu, Chem. Phys. Lett. 10, 322 (1971).
[16]C. F. Bender and H. F. Schaefer, III, J. Mol. Spectrosc. 37, 423 (1971).
[17]S. Bell, J. Chem. Phys. 68, 3014 (1978).
[18]T. H. Dunning, Jr., J. Chem. Phys. 53, 2823 (1970).
[19]S. Huzinaga, J. Chem. Phys. 42, 1293 (1965).
[20]M. Urban, V. Kellö, and I. Hubač, Chem. Phys. Lett. 51, 170 (1977).